

Optimal inference of a generalised Potts model by single-layer transformers with factored attention

Riccardo Rende, Federica Gerace, Alessandro Laio, and Sebastian Goldt*

Scuola Internazionale Superiore di Studi Avanzati (SISSA), Via Bonomea 265, 34136 Trieste, Italy

(Dated: April 17, 2023)

Transformers are the type of neural networks that has revolutionised natural language processing and protein science. Their key building block is a mechanism called self-attention which is trained to predict missing words in sentences. Despite the practical success of transformers in applications it remains unclear what self-attention learns from data, and how. Here, we give a precise analytical and numerical characterisation of transformers trained on data drawn from a generalised Potts model with interactions between sites and Potts colours. While an off-the-shelf transformer requires several layers to learn this distribution, we show analytically that a single layer of self-attention with a small modification can learn the Potts model exactly in the limit of infinite sampling. We show that this modified self-attention, that we call “factored”, has the same functional form as the conditional probability of a Potts spin given the other spins, compute its generalisation error using the replica method from statistical physics, and derive an exact mapping to pseudo-likelihood methods for solving the inverse Ising and Potts problem.

Introduction. Transformers [1] are a powerful type of neural network that have achieved state-of-the-art results in many domains: first in natural language processing (NLP) [2–6], then in protein structure prediction [7]. While standard neural networks can be thought of as functions of a single input, transformers act on sets of “tokens”, like words in a sentence. Key to their success is a technique called masked language modelling (MLM), where transformers are trained to predict missing words in a sentence [2–6], cf. fig. 1a. This technique has the advantage that it can leverage large amounts of raw text without any annotation. By learning the conditional distribution of having a word in a specific position of the sentence, given the other words, transformers ostensibly “learn” the relationships between words in a robust way.

The basic building block of transformers is the *self-attention* (SA) mechanism [8, 9], which transforms a sequence of tokens \mathbf{x}_j into another sequence \mathbf{h}_j . We illustrate self-attention on a masked language modelling task in fig. 1. The sentence is first transformed into a set of representations $\mathbf{x}_j = \mathbf{e}_j + \mathbf{p}_j$, where \mathbf{e}_j is a vector representing the j th word and the vector \mathbf{p}_j encodes the position. SA then computes a linear transformation of the representations to yield the values \mathbf{v}_j . The k th output vector \mathbf{h}_k is then a linear combination of the values \mathbf{v}_j weighted by an attention matrix A , whose elements A_{kj} quantify the relative importance of the j th input token for the k th output vector, for example based on their semantic similarity. The functions to compute values \mathbf{v}_j and the attention matrix A both have trainable parameters, see eq. (2) for a precise definition. The flexibility of self-attention comes from the attention weights A_{kj} , which are not fixed, but computed given the current context, i.e. the surrounding tokens.

The practical success of transformers raises several fundamental questions: what are the statistical structures that self-attention learns with MLM? How many sam-

ples are required to achieve good performance?

Here, we extend the statistical physics of learning [10–13] to study transformers trained using MLM. The first challenge is to design a data model that mimics the structure of sentences. While classical works modelled inputs as vectors of i.i.d. random variables, recent work has highlighted the importance of data structure for neural networks [14–20]. We model sequences using a generalised Potts model [21, 22] with interactions between colours (=words) and positions along the sequence. While a vanilla transformer requires many layers of self-attention to learn this simple probability distribution, we show an-

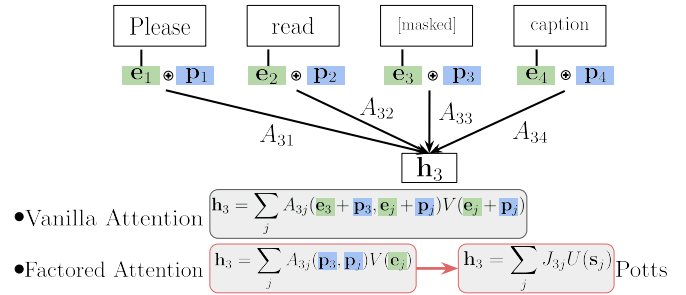


FIG. 1. **Masked language modelling (MLM) with a single layer of self-attention.** The goal of MLM is to predict the masked word in a given sentence. Self-attention first maps words into representations $\mathbf{e}_j + \mathbf{p}_j$, where \mathbf{e}_j are embedding vectors representing words, and \mathbf{p}_j encode their positions. For a given masked word, the associated attention vector \mathbf{h}_k is computed as a linear combination of the values $\mathbf{v}_j = V(\mathbf{e}_j + \mathbf{p}_j)$ of all other tokens, weighted by the attention weights A_{kj} . In vanilla self-attention, values and attention weights depend on embeddings *and* positional vectors, while in *factored* attention, attention weights depend only on positions, and values only on the embeddings. By identifying the attention weights A with the interaction matrix J of a Potts model eq. (1), the value matrix V with the colour similarity matrix U and the embedding vectors with the one-hot spins, we get a learning model identical to a Potts model.

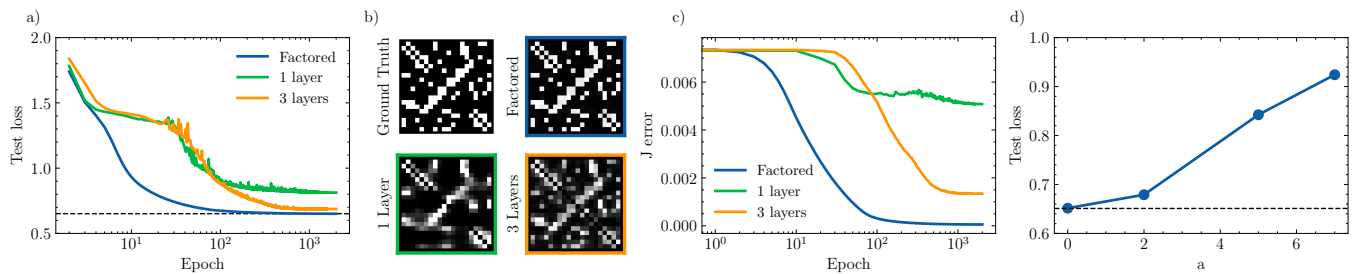


FIG. 2. **A single layer of factored self-attention learns the generalised Potts model efficiently.** (a) Test loss (3) for factored self-attention and for vanilla transformers with one and three layers during training with stochastic gradient descent. The optimal generalisation loss is shown as a black dashed line. (b) Interaction matrix J of the generative Potts Model (1) compared to the attention maps learned by transformers with vanilla and factored self-attention. For the three-layer transformer, the attention map was obtained by averaging the maps of the last two layers. (c) Reconstruction error of the interaction $(J - A)^2$ as a function of the number of epochs for all considered architectures. (d) Test error as a function of perturbation level a . Decoupling the treatment between positions and colours by decreasing a decreases the test loss. *Parameters:* embedding dimension $d = 20$, vocabulary size $C = 20$, $M = 3000$ data points, sequence length $L = 20$.

the generalised Potts model, which is

$$p(s_{i\alpha} = 1 | \mathbf{s}_i) = \frac{\exp\left(\beta \sum_{j=1}^L J_{ij}(U\mathbf{s}_j)_\alpha\right)}{\sum_{\gamma=1}^C \exp\left(\beta \sum_{j=1}^L J_{ij}(U\mathbf{s}_j)_\gamma\right)}, \quad (5)$$

if one sets $U = V$ and $\beta J = A$. This equivalence between factored self-attention and the Potts model is our first main result; we now discuss its ramifications.

Decoupling positions and colours leads to a significant improvement in the performance of a single layer, which reaches the optimal generalisation error and converges faster, cf. fig. 2a. Factored self-attention recovers the interaction matrix J perfectly, cf. fig. 2b for the attention map and fig. 2c for the reconstruction error of the interaction matrix. In fig. 2d, we show that decoupling the treatment of positions and colours completely performs better than some intermediate solution with $a > 0$.

The improved performance of factored self-attention is not an artefact of sampling data from the Potts model (1): Bhattacharya *et al.* [25] used this trick to analyse protein sequences and found that a single layer of factored self-attention performed as well as a deep transformer, and significantly better than a single layer of vanilla self-attention, without explaining this observation. Input-independent and translation-invariant attention weights improved the performance of transformers in computer vision [26], and got excellent results in approximating ground states of many-body quantum systems [27].

We also note that MLM with factored self-attention yields exactly the same loss as the pseudo-likelihood method for solving the inverse Ising problem [28–32]. The pseudo-likelihood method is statistically consistent [33–35], i.e. its parameter estimates converge to the true parameters as the number of samples goes to infinity. A direct consequence of the mapping in eq. (4) is thus that MLM with factored self-attention enjoys the same asymptotic optimality.

The sample complexity of self-attention. A key quantity in machine learning problems is the sample complexity, namely how many samples are required to achieve a small generalisation loss ϵ_g with a given model. The mapping in eq. (4) allows addressing this question rigorously for a single layer of self-attention by means of the replica method from statistical physics. The main difficulty in the calculation lies in handling the non-trivial data distribution (1). This difficulty can be mitigated thanks to recent advances in statistical physics, allowing the extension of replica theory to structured data [17, 19, 36]. To perform the replica calculation, we first relax the discrete nature of Potts spins by re-writing the generalised Potts Hamiltonian (1) in terms of spin magnetisation $\mathbf{m} = \langle \mathbf{s} \rangle_{P(\mathbf{s})}$ following mean-field theory. The associated Boltzmann measure then turns into a multivariate Gaussian distribution, whose covariance matrix is the negative inverse of the interaction matrix, i.e. $\Sigma = -J^{-1}$ [37, 38]. We then draw sequences $\{\mathbf{m}^\mu\}_{\mu=1}^M$ of length L from the multivariate Gaussian with zero mean and covariance matrix $\Sigma = (\Omega L^{-1/2} + \nu \mathbb{I})^{-1}$, where Ω is a symmetric full-rank random matrix sampled from the Gaussian Orthogonal ensemble while $\nu \mathbb{I}$ is a diagonal matrix centering the spectrum of Ω in ν . To ensure Σ to be positive definite, we set $\nu > 2$ due to the semicircle law [39]. By fixing the location i of the masked spin across all input sequences, solving the MLM task is equivalent to inferring the i th row of the interaction matrix \mathbf{J}_i . To accomplish this task, we train a single layer of factored self-attention by empirical risk minimisation of a square loss with ℓ_2 -regularisation:

$$\hat{\mathbf{A}}_i = \underset{\mathbf{A}_i}{\operatorname{argmin}} \left[\frac{1}{2} \sum_{\mu=1}^M \left(m_i^\mu - \mathbf{A}_i \cdot \mathbf{m}_i^\mu \right)^2 + \frac{\lambda}{2} \|\mathbf{A}_i\|_2^2 \right]. \quad (6)$$

Our goal is to characterise the generalisation loss ϵ_g (3). In the high-dimensional limit, where the number of samples and the sequence length $M, L \rightarrow \infty$

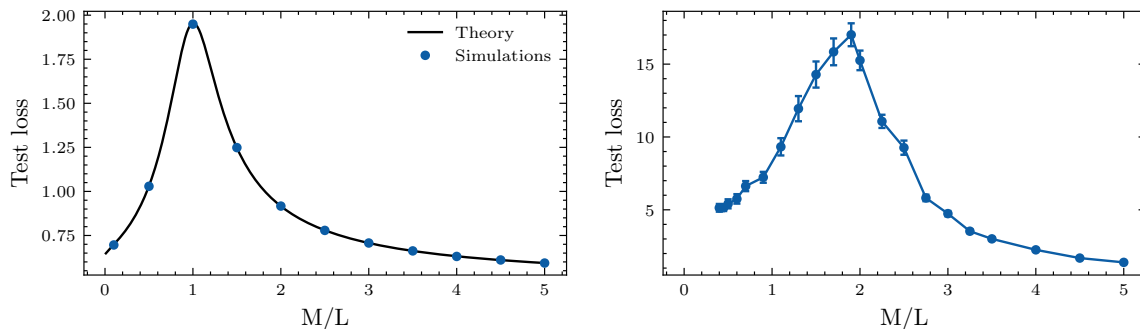


FIG. 3. **The interpolation peak of factored attention in theory and practice.** (Left) A replica analysis predicts the test error exactly. Test error of a single layer of factored self-attention as a function of the number of samples per input dimension, as computed using replica theory (solid line). The blue points represent the outcome of numerical minimisation of the square loss (6), averaged over 30 realisations, and show perfect agreement with the theory. Error bars are smaller than point size. (Right) Same plot for a single layer of factored self-attention in the setting of fig. 2 ($L = C = 20$), showing the same qualitative behaviour. The simulations are averaged over $n = 30$ different realisations.

while $\alpha \equiv M/L \sim O(1)$, we can express ϵ_g using replica theory as a function of only scalar quantities,

$$\epsilon_g = \rho + q^* - 2r^* + 1/\nu. \quad (7)$$

Here, $\rho = \text{tr}\Sigma_{\setminus i}/(\nu^2 L)$ is a function of the covariance matrix $\Sigma_{\setminus i}$ where we have removed the i th row and column, while q^* and r^* are the so-called overlap parameters. As we show in the supplementary material, the values of these order parameters for a given training set size α can be obtained by solving the optimisation problem

$$f_\beta = \text{extr}_{q,r,l,\hat{q},\hat{r},\hat{l}} \left[-\frac{1}{2} (\hat{q}l - q\hat{l}) + \nu r \hat{r} + \lim_{L \rightarrow \infty} \frac{1}{L} \Psi_s + \alpha \Psi_e \right] \quad (8)$$

which yields the *typical* value (over the data) of the free energy density associated to a Gibbs measure at inverse temperature β whose Hamiltonian corresponds to the loss function in eq. (6). Note that the optimisation only involves the scalar parameters q , r , l and their conjugates \hat{q} , \hat{r} and \hat{l} . The entropic and energetic potentials Ψ_s and Ψ_e are both functions of $\Sigma_{\setminus i}$ and are given in the SM.

We plot the resulting generalisation loss as a function of the rescaled number of samples $\alpha \equiv M/L$ on the right of fig. 3. The test loss actually *increases* when adding more training sequences to a small data set, before peaking at $\alpha = 1$. Below this threshold, the model overfits to its training data; beyond this threshold, the generalisation error decreases monotonically with the training set size; for large α , we found $\epsilon_g \sim \alpha^{-1/2}$. A similar peak in the generalization loss has been observed in supervised learning [40] and it is connected to the well-known “double descent” curve observed in deep neural networks in the presence of label noise [41]. There, the peak is a consequence of overfitting and it appears after an initial decay of the test loss at small α . In MLM, we find instead that the peak appears naturally as a consequence of the intrinsic stochasticity of the inputs, which also causes the absence of an initial decay of the loss due to the high level of noise in the labels.

We verified the predictions of replica theory by plotting the generalisation loss of a single layer of factored self-attention trained on the generalised Potts Model in the setting of fig. 2 at small regularisation (right of fig. 3). We see the same qualitative behaviour as predicted by replica theory, even though in this case we did not apply any of the assumptions required for the replica analysis (the mean field limit, the usage of a full-rank J matrix and of a U matrix fixed to the identity). In particular, the test loss increases when adding more data for small α . The only difference between the plots is the location of the peak. For the square loss that we analysed with replicas, it appears at the interpolation threshold, which is the largest number of samples that the neural network can fit perfectly, which is at $M = L$ for a system of linear equations. For the simulations with logistic loss, the peak appears at the linearly separability threshold, which is the largest number of points a linear classifier can classify correctly, and which can be larger than one [10, 17].

Concluding perspectives. We provided an analytical and numerical characterization of self-attention trained on data sampled from a generalised Potts model with two-body interactions between both sites and colours. We showed that training factored self-attention on the MLM objective is equivalent to solving the inverse Potts problem using the pseudo-likelihood method [28–32], and therefore yields consistent estimators of the parameters.

Learning higher-order interactions will require additional layers: a detailed study of how this can be achieved is an interesting direction for future research. Our replica analysis of self-attention enabled us to compute the generalisation loss of the model exactly and yielded a new type of generalisation behaviour. It will be interesting to also study the learning *dynamics* using methods from statistical physics [42–45], both on MLM and on supervised tasks [46–49]. Finally, our work clarifies the limits of standard self-attention trained on data where two-body interactions dominate and highlights the potential of factored attention as a component of transformer models.

We thank Marc Mézard and Lenka Zdeborová for stimulating discussions, and Santiago Acevedo for critically reading the manuscript.

* sgoldt@sissa.it

- [1] A. Vaswani, N. Shazeer, *et al.*, Advances in neural information processing systems (2017).
- [2] J. Devlin, M.-W. Chang, K. Lee, and K. Toutanova, arXiv preprint arXiv:1810.04805 (2018).
- [3] J. Howard and S. Ruder, in *Proceedings of the 56th Annual Meeting of the Association for Computational Linguistics* (2018).
- [4] A. Radford, K. Narasimhan, *et al.*, “Improving language understanding by generative pre-training,” (2018), preprint.
- [5] T. Brown, B. Mann, *et al.*, Advances in neural information processing systems (2020).
- [6] OpenAI, arXiv preprint arXiv:2303.08774v2 (2023).
- [7] J. Jumper, R. Evans, *et al.*, Nature (2021).
- [8] D. Bahdanau, K. Cho, and Y. Bengio, in *ICLR* (2015).
- [9] Y. Kim, C. Denton, L. Hoang, and A. M. Rush, in *International Conference on Learning Representations* (2017).
- [10] E. Gardner and B. Derrida, Journal of Physics A: Mathematical and General (1989).
- [11] H. S. Seung, H. Sompolinsky, and N. Tishby, Physical review A (1992).
- [12] A. Engel and C. Van den Broeck, *Statistical mechanics of learning* (2001).
- [13] G. Carleo, I. Cirac, K. Cranmer, L. Daudet, M. Schuld, N. Tishby, L. Vogt-Maranto, and L. Zdeborová, Rev. Mod. Phys. (2019).
- [14] S. Chung, D. D. Lee, and H. Sompolinsky, Phys. Rev. X (2018).
- [15] S. Goldt, M. Mézard, F. Krzakala, and L. Zdeborová, Physical Review X (2020).
- [16] S. Spigler, M. Geiger, and M. Wyart, Journal of Statistical Mechanics: Theory and Experiment (2020).
- [17] F. Gerace, B. Loureiro, F. Krzakala, M. Mézard, and L. Zdeborová, in *International Conference on Machine Learning* (2020).
- [18] A. Favero, F. Cagnetta, and M. Wyart, Advances in Neural Information Processing Systems (2021).
- [19] B. Loureiro, C. Gerbelot, H. Cui, S. Goldt, F. Krzakala, M. Mezard, and L. Zdeborová, in *Advances in Neural Information Processing Systems* (2021).
- [20] A. Ingrosso and S. Goldt, Proceedings of the National Academy of Sciences (2022).
- [21] R. B. Potts, Mathematical Proceedings of the Cambridge Philosophical Society (1952).
- [22] F.-Y. Wu, Reviews of modern physics (1982).
- [23] For a vector $\mathbf{x} = (x_i)$, the softmax non-linearity yields $x'_i = \exp(x_i) / \sum_j \exp(x_j)$. The elements of \mathbf{x}' can be interpreted as a probability distribution, since they are positive and sum to one.
- [24] R. D. Finn, A. Bateman, *et al.*, Nucleic acids research (2014).
- [25] N. Bhattacharya, N. Thomas, *et al.*, bioRxiv:2020.12.21.423882 (2020).
- [26] Z. Dai, H. Liu, Q. V. Le, and M. Tan, Advances in Neural Information Processing Systems (2021).
- [27] L. L. Viteritti, R. Rende, and F. Becca, “Transformer variational wave functions for frustrated quantum spin systems,” (2022), arXiv:2211.05504.
- [28] J. Besag, Journal of the Royal Statistical Society: Series D (The Statistician) (1975).
- [29] S. Cocco and R. Monasson, Physical review letters (2011).
- [30] F. Ricci-Tersenghi, Journal of Statistical Mechanics: Theory and Experiment (2012).
- [31] M. Ekeberg, C. Lövkvist, Y. Lan, M. Weigt, and E. Aurell, Phys. Rev. E (2013).
- [32] S. Cocco, C. Feinauer, *et al.*, Reports on Progress in Physics (2018).
- [33] A. Hyvärinen, Neural Computation (2006).
- [34] P. Ravikumar, M. J. Wainwright, and J. D. Lafferty, Ann. Statist. (2010).
- [35] E. Aurell and M. Ekeberg, Physical review letters (2012).
- [36] S. Goldt, B. Loureiro, G. Reeves, F. Krzakala, M. Mézard, and L. Zdeborová, in *Mathematical and Scientific Machine Learning* (2022).
- [37] F. Morcos, A. Pagnani, B. Lunt, A. Bertolino, D. S. Marks, C. Sander, R. Zecchina, J. N. Onuchic, T. Hwa, and M. Weigt, Proceedings of the National Academy of Sciences (2011).
- [38] H. C. Nguyen, R. Zecchina, and J. Berg, Advances in Physics (2017).
- [39] G. Livan, M. Novaes, and P. Vivo, Monograph Award (2018).
- [40] M. Opper and W. Kinzel, Models of Neural Networks III: Association, Generalization, and Representation (1996).
- [41] P. Nakkiran, G. Kaplun, *et al.*, Journal of Statistical Mechanics: Theory and Experiment (2021).
- [42] D. Saad and S. Solla, Phys. Rev. Lett. (1995).
- [43] M. Biehl and H. Schwarze, J. Phys. A. Math. Gen. (1995).
- [44] S. Goldt, M. S. Advani, A. M. Saxe, F. Krzakala, and L. Zdeborová, Journal of Statistical Mechanics: Theory and Experiment (2020).
- [45] R. Veiga, L. Stephan, B. Loureiro, F. Krzakala, and L. Zdeborova, in *Advances in Neural Information Processing Systems*.
- [46] C. Zhang, M. Raghu, J. Kleinberg, and S. Bengio, arXiv:2107.12580 (2021).
- [47] Y. Zhang, A. Backurs, S. Bubeck, R. Eldan, S. Gunasekar, and T. Wagner, arXiv:2206.04301 (2022).
- [48] E. Abbe, S. Bengio, E. Cornacchia, J. Kleinberg, A. Lotfi, M. Raghu, and C. Zhang, in *Advances in Neural Information Processing Systems* (2022).
- [49] A. Seif, S. A. Loos, G. Tucci, É. Roldán, and S. Goldt, arXiv:2205.14683 (2022).
- [50] J. Bradbury, R. Frostig, P. Hawkins, M. J. Johnson, C. Leary, D. Maclaurin, G. Necula, A. Paszke, J. VanderPlas, S. Wanderman-Milne, and Q. Zhang, “JAX: composable transformations of Python+NumPy programs,” (2018).
- [51] P. Lippe, “UvA Deep Learning Tutorials,” <https://uvadlc-notebooks.readthedocs.io/en/latest/> (2022).

APPENDIX

Numerical details

The numerical simulations were performed using JAX [50]. Both the *factored* attention layer and the vanilla transformer architecture were optimised using SGD with mini-batch size of 100 and a cosine annealer as the learning rate decay scheduler, both standard choices in the literature. The initial learning rate was adjusted to the specific simulations, choosing it between 0.1 and 0.01. The vanilla transformer code has been taken from the notebook [51], with no modifications made. In particular, as already pointed out in the main text, each element \mathbf{s}_i of a sequence $\mathbf{s} = (\mathbf{s}_1, \dots, \mathbf{s}_L)$ is first transformed into a token $\mathbf{x}_i = \mathbf{e}_i + \mathbf{p}_i$, with \mathbf{e}_i being the embedding of \mathbf{s}_i and \mathbf{p}_i being the positional encoding. The tokenized sequences are then fed to a layer made of two distinct sub-layers. The first sub-layer is composed of a single-head attention, instead the second sub-layer contains a two layer fully connected neural network. The inputs of both sublayers are connected to their outputs through skip-connections, and layer normalization is then applied.

Finally, there is an output layer consisting of a linear transformation from the d - to the C -dimensional space, in order to obtain a probability distribution over the colours through the *softmax* non-linearity. For a graphic visualization of the transformer encoder architecture, reference can be made to the original paper of Vaswani *et al.* [1]. Below is the list of transformer hyperparameters used for the simulations of fig. 2: embedding dimension 20, number of heads 1, number of layers 1-3, dropout probability 0.0, number of classes 20.

The dataset was generated using Gibbs sampling, starting from a random sequence of $L = 20$ sites and $C = 20$ Potts colors and cyclically sampling the spins by exploiting the knowledge of the exact conditional probabilities, eq. (5). In order to decorrelate the samples, 10000 Gibbs sweeps were made between each two saved configurations.

The simulations on the left panel of fig. 3, have been performed by sampling the input data-points from a multivariate Gaussian distribution and the masked token from the same distribution, conditioned on the other elements in the sequence. The optimization problem in eq. (6) is then solved in closed-form thanks to the Moore-Penrose inverse as in [17].

Replica analysis of self-attention

In this section we discuss the replica analysis of a factored single layer self-attention in detail. The computation builds upon the recent advances in statistical physics of learning, concerning the extension of replica theory to structured data [17, 19, 36]. In the following we will show how to slightly modify this new approach in order to deal with masked language modelling tasks, under the following simplified assumptions: mean-field limit, full-rank \mathbf{J} matrix, \mathbf{U} matrix fixed to the identity and thus not learned.

Statistical physics formulation of machine learning problems

Statistical physics considers learning as a dynamical and exploratory process across the space of the learnable parameters. At equilibrium, these parameters are assumed to follow a Boltzmann-Gibbs distribution, where the role of the Hamiltonian is actually played by the loss function:

$$\pi_\beta(\mathbf{A}_i, \mathcal{D}) = \frac{P(\mathbf{A}_i)}{\mathcal{Z}_\beta} e^{-\beta \sum_{\mu=1}^M \ell\left(m_i^\mu, \frac{\mathbf{A}_i \cdot \mathbf{m}_i^\mu}{\sqrt{L}}\right)} = \frac{P_A(\mathbf{A}_i)}{\mathcal{Z}_\beta} \prod_{\mu=1}^M P_G\left(m_i^\mu \mid \frac{\mathbf{A}_i \cdot \mathbf{m}_i^\mu}{\sqrt{L}}\right) \quad (9)$$

with β being the inverse temperature and \mathcal{D} the training set. In the zero temperature limit (i.e. $\beta \rightarrow \infty$), the Boltzmann-Gibbs distribution concentrates around the minima of the loss function, which are nothing but the solutions of the optimization problem in eq. 6:

$$\hat{\mathbf{A}}_i \underset{\beta \rightarrow \infty}{=} \mathbb{E}_{\pi_\beta}[\mathbf{A}_i] \quad (10)$$

Up to this point, re-framing a machine learning problem in terms of statistical physics does not seem to be a great advantage since sampling from an high-dimensional Boltzmann-Gibbs distribution is known to be impracticable.

This is where the replica theory comes into play. In particular, it states that, in the high-dimensional limit (i.e. $M, L \rightarrow \infty$ with $\alpha \equiv M/L \sim O(1)$) the free-energy of a learning system concentrates around its typical value over the input data distribution:

$$f_\beta = - \lim_{L \rightarrow \infty} \frac{1}{L} \mathbb{E}_{\{\mathbf{m}_{\setminus i}^\mu, m_i^\mu\}} [\log \mathcal{Z}_\beta]. \quad (11)$$

As we will see in the next section, this expectation can be tackled by means of the replica trick. From this quantity, all the high-dimensional metrics of interests, can be computed as a function of simple scalar quantities. This is for instance the case of the generalization loss in eq. (7). In particular, the overlap parameters m_\star and q_\star correspond to practically measurable quantities over different realisation of the training set, involving the estimator of the i th row of the interaction matrix:

$$q^\star = \frac{\hat{\mathbf{A}}_i^t \Sigma_{\setminus i} \hat{\mathbf{A}}_i}{L} \quad r^\star = - \frac{\mathbf{J}_i^t \Sigma_{\setminus i} \hat{\mathbf{A}}_i}{\nu L}. \quad (12)$$

In the next section we will outline the main steps of the replica trick leading to the generalization loss formula in eq. (7).

Replica Calculation

As anticipated in the previous section, the replica trick allows to compute the typical value of the free-energy density in eq. (11) by expressing this quantity as a function of the solely replicated partition function \mathcal{Z}_β^n , obtained by constructing $n > 0$ different and independent copies of the same learning system:

$$f_\beta = - \lim_{n \rightarrow 0^+} \frac{d}{dn} \lim_{L \rightarrow \infty} \left[\frac{1}{L} \mathbb{E}_{\{\mathbf{m}_{\setminus i}^\mu, m_i^\mu\}} \mathcal{Z}_\beta^n \right]. \quad (13)$$

Average over the training set. As a first step, the replica calculation focuses on the expectation of the replicated partition function over the training set, which, written in a more explicit form, looks like:

$$\mathbb{E}_{\{\mathbf{m}_{\setminus i}^\mu, m_i^\mu\}} \mathcal{Z}_\beta^n = \mathbb{E}_{\{m_i^\mu | \mathbf{m}_{\setminus i}^\mu\}} \mathbb{E}_{\mathbf{m}_{\setminus i}^\mu} \left[\int \prod_{a=1}^n d\mathbf{A}_i^a \prod_{a=1}^n P_A(\mathbf{A}_i^a) \prod_{\mu=1}^M P_G \left(m_i^\mu \mid \frac{\mathbf{A}_i^a \cdot \mathbf{m}_{\setminus i}^\mu}{\sqrt{L}} \right) \right], \quad (14)$$

with P_G and P_A being respectively the Gibbs and the Gaussian measure associated to the i th row of the attention matrix as in eq. (9). Indeed, as already pointed out in the main manuscript, the interaction matrix is drawn from the Gaussian Orthogonal Ensemble, therefore its rows will correspond to Gaussian random vectors. At this point, we can notice an important aspect of MLM tasks. In this case, the labels are not provided by a teacher vector as in standard teacher-student settings. On the contrary, the masked tokens are directly sampled from the input distribution by conditioning over all the other elements composing the sequence:

$$m_i^\mu \sim \frac{P_J(\mathbf{J}_i)}{\sqrt{2\pi\nu^{-1}}} e^{-\frac{1}{2\nu^{-1}} \left(m_i^\mu + \frac{\mathbf{J}_i \cdot \mathbf{m}_{\setminus i}^\mu}{\nu\sqrt{L}} \right)^2} = P_J(\mathbf{J}_i) P_0 \left(m_i^\mu \mid \frac{\mathbf{J}_i \cdot \mathbf{m}_{\setminus i}^\mu}{\nu\sqrt{L}} \right). \quad (15)$$

Note that, the noise in the labels arises a consequence of the one already affecting the input data points, meaning that its intensity can not be chosen independently from the intrinsic stochasticity of the input. Due to these considerations, by explicitly expressing the outer expectation in eq. (14), we then get:

$$\begin{aligned} \mathbb{E}_{\{\mathbf{m}_{\setminus i}^\mu, m_i^\mu\}} \mathcal{Z}_\beta^n &= \int d\mathbf{J}_i P_J(\mathbf{J}_i) \int \prod_{a=1}^n d\mathbf{A}_i^a \prod_{a=1}^n P_A(\mathbf{A}_i^a) \times \\ &\times \int dm_i^\mu \mathbb{E}_{\mathbf{m}_{\setminus i}^\mu} \left[\prod_{\mu=1}^M P_0 \left(m_i^\mu \mid \frac{\mathbf{J}_i \cdot \mathbf{m}_{\setminus i}^\mu}{\nu\sqrt{L}} \right) P_G \left(m_i^\mu \mid \frac{\mathbf{A}_i^a \cdot \mathbf{m}_{\setminus i}^\mu}{\sqrt{L}} \right) \right]. \end{aligned} \quad (16)$$

To compute the expectation over the input sequences with a masked element at position i , we first define the pre-activations as:

$$h_a^\mu = \frac{\mathbf{A}_i^a \cdot \mathbf{m}_{\setminus i}^\mu}{\sqrt{L}} \quad z^\mu = -\frac{\mathbf{J}_i \cdot \mathbf{m}_{\setminus i}^\mu}{\nu\sqrt{L}}, \quad (17)$$

then we express these definitions in terms of Dirac-deltas and their corresponding integral representation:

$$\begin{aligned} 1 &\propto \int \prod_{\mu=1}^M \prod_{a=1}^n dh_a^\mu \delta \left(h_a^\mu - \frac{\mathbf{A}_i^a \cdot \mathbf{m}_{\setminus i}^\mu}{\sqrt{L}} \right) = \int \prod_{\mu=1}^M \prod_{a=1}^n \frac{dh_a^\mu d\hat{h}_a^\mu}{2\pi} \prod_{\mu=1}^M e^{i\hat{h}_a^\mu \left(h_a^\mu - \frac{\mathbf{A}_i^a \cdot \mathbf{m}_{\setminus i}^\mu}{\sqrt{L}} \right)} \\ 1 &\propto \int \prod_{\mu=1}^M dz^\mu \delta \left(z^\mu + \frac{\mathbf{J}_i \cdot \mathbf{m}_{\setminus i}^\mu}{\nu\sqrt{L}} \right) = \int \prod_{\mu=1}^M \frac{dz^\mu d\hat{z}^\mu}{2\pi} \prod_{\mu=1}^M e^{i\hat{z}^\mu \left(z^\mu + \frac{\mathbf{J}_i \cdot \mathbf{m}_{\setminus i}^\mu}{\nu\sqrt{L}} \right)}. \end{aligned} \quad (18)$$

By plugging these factors one into eq. (16), we then get:

$$\begin{aligned} \mathbb{E}_{\{\mathbf{m}_{\setminus i}^\mu, m_i^\mu\}} \mathcal{Z}_\beta^n &= \int d\mathbf{J}_i P_J(\mathbf{J}_i) \int \prod_{a=1}^n d\mathbf{A}_i^a \prod_{a=1}^n P_A(\mathbf{A}_i^a) \times \\ &\times \int \prod_{\mu=1}^M dm_i^\mu \int \prod_{\mu=1}^M \frac{dz^\mu d\hat{z}^\mu}{2\pi} \prod_{\mu=1}^M e^{i\hat{z}^\mu z^\mu} \prod_{\mu=1}^M P_0(m_i^\mu | z^\mu) \times \\ &\times \int \prod_{\mu=1}^M \prod_{a=1}^n \frac{dh_a^\mu d\hat{h}_a^\mu}{2\pi} \prod_{\mu=1}^M \prod_{a=1}^n e^{i\hat{h}_a^\mu h_a^\mu} \prod_{\mu=1}^M \prod_{a=1}^n P_G(m_i^\mu | h_a^\mu) \times \\ &\times \prod_{\mu=1}^n \mathbb{E}_{\mathbf{m}_{\setminus i}^\mu} \left[e^{i\hat{z}^\mu \frac{\mathbf{J}_i \cdot \mathbf{m}_{\setminus i}^\mu}{\nu\sqrt{L}}} \prod_{a=1}^n e^{-i\hat{h}_a^\mu \frac{\mathbf{A}_i^a \cdot \mathbf{m}_{\setminus i}^\mu}{\sqrt{L}}} \right]. \end{aligned} \quad (19)$$

The expectation over the masked input sequences is a simple multivariate Gaussian integral, whose solution is given by:

$$\mathbb{E}_{\mathbf{m}_{\setminus i}^\mu} \left[e^{i\hat{z}^\mu \frac{\mathbf{J}_i \cdot \mathbf{m}_{\setminus i}^\mu}{\nu\sqrt{L}}} \prod_{a=1}^n e^{-i\hat{h}_a^\mu \frac{\mathbf{A}_i^a \cdot \mathbf{m}_{\setminus i}^\mu}{\sqrt{L}}} \right] = e^{-\frac{1}{2} \frac{\mathbf{J}_i^\dagger \Sigma_{\setminus i} \mathbf{J}_i}{\nu^2 L} (z^\mu)^2 + \sum_{a=1}^n \frac{\mathbf{J}_i^\dagger \Sigma_{\setminus i} \mathbf{A}_i^a}{\nu L} \hat{h}_a^\mu z^\mu - \frac{1}{2} \sum_{a,b=1}^n \frac{(\mathbf{A}_i^a)^\dagger \Sigma_{\setminus i} \mathbf{A}_i^b}{L} \hat{h}_a^\mu \hat{h}_b^\mu} \quad (20)$$

where, as already pointed out in the main text, $\Sigma_{\setminus i}$ corresponds to the covariance matrix of the masked input sequences, that is the input covariance matrix without the contribution of the row and column associated to the i th masked token. By replacing the solution of the expectation in eq. (19), we then get:

$$\begin{aligned} \mathbb{E}_{\{\mathbf{m}_{\setminus i}^\mu, m_i^\mu\}} \mathcal{Z}_\beta^n &= \int d\mathbf{J}_i P_J(\mathbf{J}_i) \int \prod_{a=1}^n d\mathbf{A}_i^a \prod_{a=1}^n P_A(\mathbf{A}_i^a) \times \\ &\times \int \prod_{\mu=1}^M dm_i^\mu \int \prod_{\mu=1}^M \frac{dz^\mu d\hat{z}^\mu}{2\pi} \prod_{\mu=1}^M e^{i\hat{z}^\mu z^\mu} \prod_{\mu=1}^M P_0(m_i^\mu | z^\mu) \times \\ &\times \int \prod_{\mu=1}^M \prod_{a=1}^n \frac{dh_a^\mu d\hat{h}_a^\mu}{2\pi} \prod_{\mu=1}^M \prod_{a=1}^n e^{i\hat{h}_a^\mu h_a^\mu} \prod_{\mu=1}^M \prod_{a=1}^n P_G(m_i^\mu | h_a^\mu) \times \\ &\times \prod_{\mu=1}^n e^{-\frac{1}{2} \frac{\mathbf{J}_i^\dagger \Sigma_{\setminus i} \mathbf{J}_i}{\nu^2 L} (z^\mu)^2 + \sum_{a=1}^n \frac{\mathbf{J}_i^\dagger \Sigma_{\setminus i} \mathbf{A}_i^a}{\nu L} \hat{h}_a^\mu z^\mu - \frac{1}{2} \sum_{a,b=1}^n \frac{(\mathbf{A}_i^a)^\dagger \Sigma_{\setminus i} \mathbf{A}_i^b}{L} \hat{h}_a^\mu \hat{h}_b^\mu}. \end{aligned} \quad (21)$$

Rewriting the averaged replicated partition function in terms of saddle-point integrals. As a consequence of the average over the training set, the different replicas are now interacting among each other through the following set of overlap parameters:

$$\rho = \frac{\mathbf{J}_i^t \Sigma_{\setminus i} \mathbf{J}_i}{\nu^2 L} \quad r_a = -\frac{(\mathbf{A}_i^a)^t \Sigma_{\setminus i} \mathbf{J}_i}{\nu L} \quad q_{ab} = -\frac{(\mathbf{A}_i^a)^t \Sigma_{\setminus i} \mathbf{A}_i^b}{L}. \quad (22)$$

Once again, to proceed further in the calculation, we can insert their definition by means of Dirac-deltas and their integral representation:

$$\begin{aligned} 1 &\propto \int d\rho \delta(\nu^2 L \rho - \mathbf{J}_i^t \Sigma_{\setminus i} \mathbf{J}_i) = \int \frac{d\rho d\hat{\rho}}{2\pi} e^{i\hat{\rho}(\nu^2 L \rho - \mathbf{J}_i^t \Sigma_{\setminus i} \mathbf{J}_i)} \\ 1 &\propto \int \prod_{a=1}^n dr_a \delta(-\nu L r_a - (\mathbf{A}_i^a)^t \Sigma_{\setminus i} \mathbf{J}_i) = \int \prod_{a=1}^n \frac{dr_a d\hat{r}_a}{2\pi} \prod_{a=1}^n e^{i\hat{r}_a(-\nu L r_a - (\mathbf{A}_i^a)^t \Sigma_{\setminus i} \mathbf{J}_i)} \\ 1 &\propto \int \prod_{a \leq b} dq_{ab} \delta(L q_{ab} - (\mathbf{A}_i^a)^t \Sigma_{\setminus i} \mathbf{A}_i^b) = \int \prod_{a \leq b} \frac{dq_{ab} d\hat{q}_{ab}}{2\pi} \prod_{a \leq b} e^{i\hat{q}_{ab}(q_{ab} - (\mathbf{A}_i^a)^t \Sigma_{\setminus i} \mathbf{A}_i^b)}. \end{aligned} \quad (23)$$

By substituting the overlap definition in eq. (21), plugging in the corresponding factors one and performing the change of variables: $i\hat{\rho} \rightarrow -\hat{\rho}$, $i\hat{r}_a \rightarrow \hat{r}_a$ and $i\hat{q}_{ab} \rightarrow \hat{q}_{ab}$, we can rewrite the averaged replicated partition function in terms of saddle-point integrals over the overlap parameters:

$$\mathbb{E}_{\{\mathbf{m}_{\setminus i}^\mu, m_i^\mu\}} \mathcal{Z}_\beta^n = \int \frac{d\rho d\hat{\rho}}{2\pi} \int \prod_{a=1}^n \frac{dr_a d\hat{r}_a}{2\pi} \int \prod_{a \leq b} \frac{dq_{ab} d\hat{q}_{ab}}{2\pi} e^{L\Psi^{(n)}} \quad (24)$$

where the action $\Psi^{(n)}$ is a non trivial function of the overlap parameters:

$$\Psi^{(n)} = -\nu^2 \rho \hat{\rho} + \nu \sum_{a=1}^n r_a \hat{r}_a - \sum_{a \leq b} q_{ab} \hat{q}_{ab} + \frac{1}{L} \Psi_s + \frac{M}{L} \Psi_e \quad (25)$$

where Ψ_s and Ψ_e are the so-called entropic and energetic potential and, in the specific case of a single-layer factored attention, are given by:

$$\begin{aligned} \Psi_s &= \log \left[\int d\mathbf{J}_i P_J(\mathbf{J}_i) \int \prod_{a=1}^n d\mathbf{A}_i^a P_A(\mathbf{A}_i^a) e^{\hat{\rho} \mathbf{J}_i^t \Sigma_{\setminus i} \mathbf{J}_i + \sum_{a=1}^n \hat{r}_a (\mathbf{A}_i^a)^t \Sigma_{\setminus i} \mathbf{J}_i + \sum_{a \leq b} \hat{q}_{ab} (\mathbf{A}_i^a)^t \Sigma_{\setminus i} \mathbf{A}_i^b} \right] \\ \Psi_e &= \log \left[\int dm_i \int \frac{dz d\hat{z}}{2\pi} e^{-\frac{\hat{z}}{2} z^2 + i\hat{z}z} P_0(m_i|z) \times \right. \\ &\quad \left. \times \int \prod_{a=1}^n \frac{dh_a d\hat{h}_a}{2\pi} e^{-\frac{1}{2} \sum_{a,b=1}^n q_{ab} \hat{h}_a \hat{h}_b - \hat{z} \sum_{a=1}^n r_a \hat{h}_a + i \sum_{a=1}^n \hat{h}_a h_a} P_G(m_i|h_a) \right]. \end{aligned} \quad (26)$$

Note that, we have drop the dependency of Ψ_e on the μ index since all the μ -dependent terms decouple with respect to μ .

Replica Symmetric Assumption. To proceed further in the calculation, we need to assume a specific replica structure. Since all replicas have been introduced independently from each other with no specific differences among them, it seems natural to assume that replicas should all play the same role and that, therefore, the overlap parameters should not depend on the specific replica index. In particular, under the replica symmetric ansatz, we assume:

$$\begin{aligned} q_{ab} &= \begin{cases} g & \text{if } a = b \\ q & \text{otherwise} \end{cases} & -i\hat{q}_{ab} &= \begin{cases} -\frac{\hat{g}}{2} & \text{if } a = b \\ \hat{q} & \text{otherwise} \end{cases} \\ r_a &= r & -i\hat{r}_a &= \hat{r} \quad \forall a \end{aligned} \quad (27)$$

By plugging the replica symmetric assumption in eq. (25)-(29) we get the following expression for the action:

$$\Psi^{(n)} = -\nu^2 \rho \hat{\rho} + \nu r \hat{r} + \frac{n}{2} (l + q) (\hat{l} - \hat{q}) - \frac{n(n-1)}{2} q \hat{q} + \frac{1}{L} \Psi_s + \frac{M}{L} \Psi_e \quad (28)$$

where the replica symmetric potentials Ψ_s and Ψ_e are given by:

$$\begin{aligned} \Psi_s &= \log \left[\int d\mathbf{J}_i P_J(\mathbf{J}_i) e^{\hat{\rho} \mathbf{J}_i^t \Sigma_{\setminus i} \mathbf{J}_i} \times \right. \\ &\quad \left. \times \int \prod_{a=1}^n d\mathbf{A}_i^a P_A(\mathbf{A}_i^a) e^{\hat{r} \sum_{a=1}^n (\mathbf{A}_i^a)^t \Sigma_{\setminus i} \mathbf{J}_i - \frac{\hat{l}}{2} \sum_{a=1}^n (\mathbf{A}_i^a)^t \Sigma_{\setminus i} \mathbf{A}_i^a + \frac{\hat{q}}{2} \sum_{a \leq b} (\mathbf{A}_i^a)^t \Sigma_{\setminus i} \mathbf{A}_i^b} \right] \\ \Psi_e &= \log \left[\int dm_i \int \frac{dz d\hat{z}}{2\pi} e^{-\frac{\rho}{2} \hat{z}^2 + i \hat{z} z} P_0(m_i|z) \times \right. \\ &\quad \left. \times \int \prod_{a=1}^n \frac{dh_a d\hat{h}_a}{2\pi} e^{-\frac{q}{2} \sum_{a,b=1}^n \hat{h}_a \hat{h}_b - \frac{\hat{l}}{2} \sum_{a=1}^n \hat{h}_a^2 - r \hat{z} \sum_{a=1}^n \hat{h}_a + i \sum_{a=1}^n \hat{h}_a h_a} P_G(m_i|h_a) \right]. \end{aligned} \quad (29)$$

where we have defined $\hat{l} = \hat{g} + \hat{q}$ and $l = g - q$. To factorise over the replica index, we can apply the Hubbard-Stratonovich transformations

$$\begin{aligned} e^{\frac{\hat{q}}{2} \sum_{a \leq b} (\mathbf{A}^a)^t \Sigma_{\setminus i} \mathbf{A}^b} &= \int \mathcal{D}\xi \exp \left(\sum_{a=1}^n (\mathbf{A}_i^a)^t (\hat{q} \Sigma_{\setminus i})^{1/2} \xi \right) \\ e^{-\frac{q}{2} \sum_{a,b=1}^n \hat{h}_a \hat{h}_b} &= \int \mathcal{D}\xi \exp \left(i \sqrt{q} \sum_{a=1}^n \hat{h}_a^2 \xi \right), \end{aligned} \quad (30)$$

with $\xi \sim \mathcal{N}(0, 1)$, on both the entropic and energetic potential, thus getting:

$$\begin{aligned} \Psi_s &= \log \left[\int d\mathbf{J}_i P_J(\mathbf{J}_i) e^{\hat{\rho} \mathbf{J}_i^t \Sigma_{\setminus i} \mathbf{J}_i} \int \mathcal{D}\xi \left(\int d\mathbf{A}_i P_A(\mathbf{A}_i) e^{\hat{r} \mathbf{A}_i^t \Sigma_{\setminus i} \mathbf{J}_i - \frac{\hat{l}}{2} \mathbf{A}_i^t \Sigma_{\setminus i} \mathbf{A}_i + \mathbf{A}_i^t (\hat{q} \Sigma_{\setminus i})^{1/2} \xi} \right)^n \right] \\ \Psi_e &= \log \left[\int dm_i \int \frac{dz d\hat{z}}{2\pi} e^{-\frac{\rho}{2} \hat{z}^2 + i \hat{z} z} P_0(m_i|z) \int \mathcal{D}\xi \left(\int \frac{dh d\hat{h}}{2\pi} e^{-\frac{1}{2} \hat{h}^2 + i \sqrt{q} \xi \hat{h} - m \hat{z} \hat{h} + i \hat{h} h} P_G(m_i|h) \right)^n \right] \end{aligned} \quad (31)$$

Zero Replica limit. By taking the limit of $n \rightarrow 0$ in eq. (28)-(31) and solving the integrals with respect to the \hat{z} and \hat{h} variables, we then get the following expression for the action potential:

$$\Psi^{(n \rightarrow 0)} = \nu r \hat{r} + \frac{1}{2} (l + q) (\hat{l} - \hat{q}) + \frac{1}{2} q \hat{q} + \frac{1}{L} \Psi_s^{(n \rightarrow 0)} + \frac{M}{L} \Psi_e^{(n \rightarrow 0)} \quad (32)$$

with the entropic and energetic potentials in the zero replicas limit given by:

$$\begin{aligned} \Psi_s^{(n \rightarrow 0)} &= \int \mathcal{D}\xi \int d\mathbf{J}_i P_J(\mathbf{J}_i) \log \left[\int d\mathbf{A}_i P_A(\mathbf{A}_i) e^{\hat{r} \mathbf{A}_i^t \Sigma_{\setminus i} \mathbf{J}_i - \frac{\hat{l}}{2} \mathbf{A}_i^t \Sigma_{\setminus i} \mathbf{A}_i + \mathbf{A}_i^t (\hat{q} \Sigma_{\setminus i})^{1/2} \xi} \right] \\ \Psi_e^{(n \rightarrow 0)} &= \int \mathcal{D}\xi \int dm_i \int \frac{dz}{\sqrt{2\pi \left(\rho - \frac{r^2}{q} \right)}} e^{-\frac{\left(z + \frac{r \sqrt{q} \xi}{\rho - \frac{r^2}{q}} \right)^2}{2 \left(\rho - \frac{r^2}{q} \right)}} P_0(m_i|z) \log \left[\int \frac{dh}{\sqrt{2\pi l}} e^{-\frac{(h + \sqrt{q} \xi)^2}{2l}} P_G(m_i|h) \right] \end{aligned} \quad (33)$$

Note that, as in standard teacher-student settings [17], in order to avoid divergent terms in this limit, the overlap ρ and its conjugate $\hat{\rho}$ need to be constrained to $\mathbb{E}_{\mathbf{J}_i} [\mathbf{J}_i^t \Sigma_{\setminus i} \mathbf{J}_i] / \nu^2$ and 0 respectively.

Typical Free-Energy density. Having determined the expression for the replicated partition function in the zero-temperature limit, we can actually compute the typical free-energy density as:

$$f_\beta = - \lim_{n \rightarrow 0^+} \frac{d}{dn} \lim_{L \rightarrow \infty} \left[\frac{1}{L} \mathbb{E}_{\{m_i^\mu, m_i^\mu\}} \mathcal{Z}_\beta^n \right] = \lim_{L \rightarrow \infty} \frac{1}{L} \int \frac{d\rho d\hat{\rho}}{2\pi} \int \frac{dr d\hat{r}}{2\pi} \int \frac{dq d\hat{q}}{2\pi} e^{L\Psi^{(n \rightarrow 0)}}. \quad (34)$$

In the high-dimensional limit, we can solve the integrals over the overlap parameters by saddle-point, thus getting:

$$f_\beta = \underset{q, r, l, \hat{q}, \hat{r}, \hat{l}}{\text{extr}} \left[\nu r \hat{r} + \frac{1}{2} (l + q) (\hat{l} - \hat{q}) + \frac{1}{2} q \hat{q} + \lim_{L \rightarrow \infty} \frac{1}{L} \Psi_s^{(n \rightarrow 0)} + \alpha \Psi_e^{(n \rightarrow 0)} \right]. \quad (35)$$

where the values of the overlap parameters extremizing the typical free-energy density can therefore be determined by solving the following system of coupled saddle-point equations:

$$\begin{cases} q = -2 \frac{\partial \Psi_s^{(n \rightarrow 0)}}{\partial l} \\ l = 2 \frac{\partial \Psi_s^{(n \rightarrow 0)}}{\partial \hat{q}} \\ r = -\frac{1}{\nu} \frac{\partial \Psi_s^{(n \rightarrow 0)}}{\partial \hat{r}} \end{cases} \quad \begin{cases} \hat{q} = 2 \frac{\partial \Psi_e^{(n \rightarrow 0)}}{\partial l} \\ \hat{l} = -2 \frac{\partial \Psi_e^{(n \rightarrow 0)}}{\partial q} \\ \hat{r} = -\frac{1}{\nu} \frac{\partial \Psi_e^{(n \rightarrow 0)}}{\partial r} \end{cases} \quad (36)$$

Up to this point, we have performed the replica calculation in full generality, without specifying neither the interaction matrix nor the loss function. In the next section, we will evaluate the typical free-energy density for the specific MLM task of eq. (6) under the simplified assumptions of sec CITE.

Zero temperature limit and Gaussian Priors. As already pointed out in the main text, the interaction matrix J is sampled from the GOE, it is then natural to assume a Gaussian prior on the i th row of the attention matrix:

$$P_A(\mathbf{A}) = \frac{1}{\sqrt{2\pi}} e^{\beta \lambda \mathbf{A}_i^t \mathbf{A}_i} \quad (37)$$

with β being the inverse temperature parameter, while λ being the L_2 regularization strength. Moreover, the optimization problem in eq. (??) optimize a square loss to solve the corresponding MLM task. This means that, the Gibbs Measure of eq. (9) associated to this task is:

$$P_G(m_i|h) \propto e^{-\frac{\beta}{2}(m_i-h)^2}. \quad (38)$$

By plugging these two specific forms of both the prior and the Gibbs measure in eq. (??) and taking the zero temperature limit as exemplified in [17, 36], we get the following expression for the typical free-energy density in the zero-temperature limit:

$$f \underset{\beta \rightarrow \infty}{=} \underset{q, r, l, \hat{q}, \hat{r}, \hat{l}}{\text{extr}} \left[\nu r \hat{r} - \frac{1}{2} (l \hat{q} - q \hat{l}) + \lim_{L \rightarrow \infty} \frac{1}{L} \Psi_s^{(n \rightarrow 0)} + \alpha \Psi_e^{(n \rightarrow 0)} \right]. \quad (39)$$

with the entropic and energetic potential given by:

$$\begin{aligned} \Psi_s^{n \rightarrow 0} &\underset{\beta \rightarrow \infty}{=} \frac{1}{2} \left[\hat{r}^2 \text{tr}(\Sigma_{\setminus i})^t \Sigma_{\setminus i} (\beta \lambda \mathbb{I} + \hat{l} \Sigma_{\setminus i})^{-1} + \hat{q} \text{tr} \Sigma_{\setminus i} (\beta \lambda \mathbb{I} + \hat{l} \Sigma_{\setminus i})^{-1} \right] \\ \Psi_e^{n \rightarrow 0} &\underset{\beta \rightarrow \infty}{=} -\frac{1}{2} \frac{\nu^{-1} + \rho + q - 2r}{1 + l} \end{aligned} \quad (40)$$

and $\rho = \text{tr} \Sigma_{\setminus i} / (\nu^2 L)$. Note that, this functional form of the typical free-energy density corresponds exactly to the one of supervised learning with noisy label and Gaussian structured data [36]. However, we should here point out again that, the variance of the noise in the labels, controlled by the shift factor ν , is a direct consequence of the intrinsic noise already affecting the input. Therefore, it can not be tuned independently from it. This is also reflected

on the slightly different functional form of the saddle-point equations in (36), which, in the zero-temperature limit with Gaussian priors and square loss, are given by:

$$\begin{cases} q = \text{tr} \left[\left(\hat{q} \Sigma_{\setminus i} + \hat{r}^2 \Sigma_{\setminus i} (\Sigma_{\setminus i})^t \right) \Sigma_{\setminus i} \left(\lambda \mathbb{I} + \hat{l} \Sigma_{\setminus i} \right)^{-2} \right] \\ l = \text{tr} \left[\left(\lambda \mathbb{I} + \hat{l} \Sigma_{\setminus i} \right)^{-1} \Sigma_{\setminus i} \right] \\ r = -\frac{\hat{r}}{\nu} \text{tr} \left[\Sigma_{\setminus i} (\Sigma_{\setminus i})^t \left(\lambda \mathbb{I} + \hat{l} \Sigma_{\setminus i} \right)^{-1} \right] \end{cases} \quad \begin{cases} \hat{q} = \frac{\nu^{-1} + \rho + q - 2r}{(1+l)^2} \\ \hat{l} = \frac{1}{1+l} \\ \hat{r} = -\frac{1}{\nu(1+l)} \end{cases} . \quad (41)$$

As in the case of supervised learning settings [17, 36], the solution of this system of coupled saddle-point equations in the zero temperature limit allows to express the generalization loss as shown in eq. of the main text, with the exception that the noise in the labels is the direct consequence of the intrinsic noise of the inputs.